

CrossMark  
click for updatesCite this: *RSC Adv.*, 2015, 5, 91001Received 9th August 2015  
Accepted 14th October 2015

DOI: 10.1039/c5ra15970a

www.rsc.org/advances

# Selective oil/water filter paper *via* a scalable one-pot hydrothermal growth of ZnO nanowires†

Yi Chen,<sup>ab</sup> Li Liu,<sup>b</sup> Hyun-Joong Chung<sup>\*b</sup> and John A. Nychka<sup>\*b</sup>

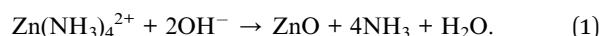
Uniform ZnO nanowires (NWs) were grown on cellulose filter paper *via* a modified one-step hydrothermal method. The ZnO coated filter paper exhibited superhydrophilicity and underwater superoleophobicity due to the surface roughness of the coated ZnO NWs. The coated cellulose filters demonstrated exceptional results at oil/water separation with high separation efficiency and experimentally proven recyclability for several oil/water mixtures. The outstanding separation performance and scalable growth method highlight potential for practical applications, such as wastewater treatment and polluted water purification.

In recent years, water cleanup by oil decontamination has been attracting extensive attention.<sup>1,2</sup> Recent studies on modulating wettability by chemical modification and/or nanoscale texturizing have achieved a remarkable enhancement in separation efficiency of oil/water suspensions.<sup>3–7</sup> However, the separated oil can cause frequent plugging of pores in the membrane, and subsequently results in low flux, low recyclability and secondary pollution.<sup>8,9</sup> An underwater oleophobicity, which means that the oil can automatically be removed from the pores when saturated with water, may provide a fundamental solution to the plugging problem. This underwater oleophobicity feature can be utilized for gravity-driven separation membranes since water usually has higher density than oil.<sup>10–15</sup>

Various approaches have been developed to achieve underwater superoleophobic surfaces. For example, free standing CNTs/TiO<sub>2</sub> network films,<sup>11</sup> graphene oxide coated membrane,<sup>12,13</sup> polydopamine/polyethylenimine modified polypropylene membranes,<sup>14</sup> and Cu(OH)<sub>2</sub> NW haired meshes<sup>15</sup> have been suggested as examples of superoleophobic membranes. Nevertheless, critical drawbacks such as high cost, low flexibility and toxicity have hindered their application in

practical applications. Hence, it remains as a challenge to develop cost-effective and scalable material processing pathways without environmentally harmful by-products so that they can be employed in large scale production and use in society.

To address these issues, we report a novel one-pot hydrothermal growth method for ZnO nanowires (NWs) that can convert a commodity filter paper into a highly efficient and reusable oil/water separating membrane. Traditional growth of ZnO NWs requires a separate step to deposit a ZnO seed layer prior to NW growth, including metal-organic chemical vapour deposition (MOCVD), chemical vapor deposition (CVD) or pulsed laser deposition.<sup>16–18</sup> In contrast to these methods, one pot methods as well as seedless ZnO growth have been receiving attention due to the potential to scale up.<sup>19,20</sup> The advantage of our method lies in an exceptional simplicity of the one-pot synthesis, which provides unmatched compatibility for scalable production. In our method, seed nucleation and growth steps are simply switched by controlling the vapour pressure over the liquid precursor solution. By increasing the roughness of the filter surface, the ZnO NW coated filter paper shows superhydrophilic and underwater superoleophobic without post treatment. The superoleophobic filter paper is free from oil fouling and has high efficiency and recyclability for oil/water separation. The ZnO NWs growth method was developed for fabrication of large scale ZnO NWs coated cellulose filter paper as illustrated in Fig. 1. Particularly, the filter paper was placed at the interface of liquid-air. When the pristine filter paper is soaked with the solution at 90 °C (Fig. 1a), the lid is removed to drop the vapor pressure to allow water and NH<sub>3</sub> gas to rapidly evaporate to form ZnO nuclei particles on the fiber surface, as described in eqn (1):<sup>21,22</sup>



The cellulose fibers in the filter paper become uniformly decorated with the nuclei particles, as shown in Fig. S1.† Once the nuclei particle layer is continuous the beaker is closed with

<sup>a</sup>Scion, Private Bag 3020, Rotorua 3046, New Zealand<sup>b</sup>Department of Chemical and Material Engineering, University of Alberta, Edmonton, Alberta, T6G 2V4, Canada. E-mail: chung3@ualberta.ca; jnychka@ualberta.ca

† Electronic supplementary information (ESI) available: Experimental section and more characterization are included. See DOI: 10.1039/c5ra15970a

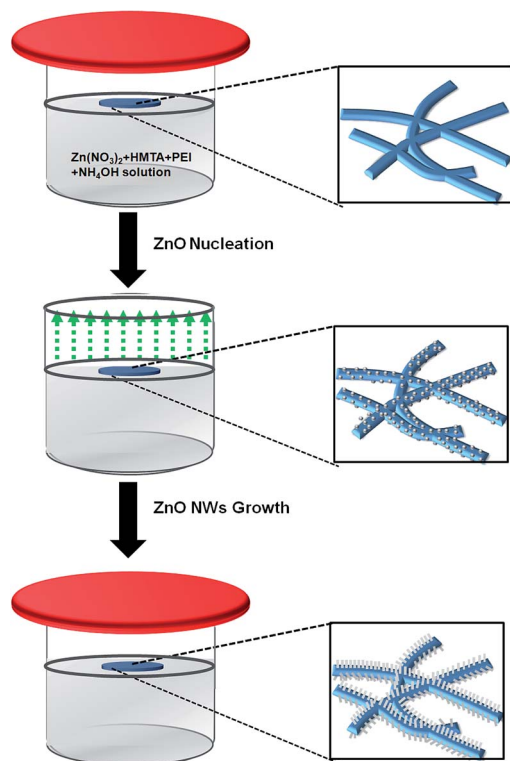


Fig. 1 A schematic illustration of the ZnO NWs growth on filter paper.

the lid again to increase the vapor pressure of ammonia and water. Now the formation of ZnO nuclei is suppressed, whereas NWs start to grow on the nuclei.<sup>15</sup> More importantly, by selective absorption on the lateral facets and chelating  $\text{Zn}^{2+}$ , polyethylenimine (PEI), a cationic polyelectrolyte, plays an essential role in controlling the NWs' length and diameter during growth by slowing down the lateral growth rate whilst maintaining the growth density and length,<sup>23,24</sup> which directly affects the surface roughness and resulting controllable wettability.<sup>25,26</sup>

Fig. 2a shows photographs of pristine (left) and ZnO NWs coated filter paper (right), indicating that there is clearly no visible difference after ZnO NW coating. In the ZnO NW coated

papers, however, XRD patterns confirm the wurtzite crystalline structure of ZnO (JCPDS no. 89-1397) (Fig. 2b). The strong and sharp diffraction peaks indicate that the ZnO NWs are highly crystalline. No other peaks besides the characteristic wurtzite ZnO pattern were detectable, except for a peak at around  $22.58^\circ$ . This extra peak corresponds to the (200) plane of cellulose.<sup>27</sup> Fig. 2c and d are the secondary electron scanning electron microscopy (SEM) images of uncoated (pristine) cellulose fibers with a typical network structure at low (Fig. 2c) and higher magnification (Fig. 2d). It is revealed that a high density of ZnO NWs were grown on the fibers with uniform diameter of 30 nm (Fig. 2f). The characterization results indicate that ZnO NWs were successfully grown on a large scale filter paper (diameter of 90 mm) and indicate that the fabrication procedure appears to be scalable.

The wetting property of the ZnO NWs coated filter paper was tested by water and oil contact angle measurements for oil and water droplets in ambient atmosphere and for oil droplets in a water environment. As shown in Fig. 3a, when a water droplet was placed onto the as-coated filter paper in ambient air (with relative humidity of 40%), the drop spread very quickly and a  $0^\circ$  contact angle was recorded (Fig. 3a), and the spread took 0.66 s, as recorded in a high-speed video for dynamic water contact angle test (Fig. S2†). The sample also exhibited  $0^\circ$  contact angle for oil in air (Fig. 3b). For underwater oil contact angle measurement, 1,2-dichloroethane (DCE) was selected as a model

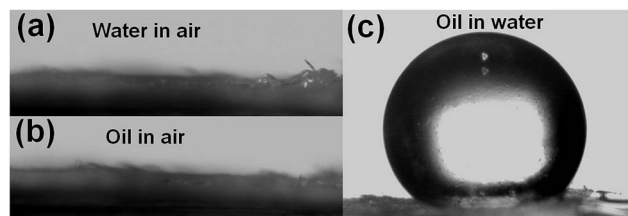


Fig. 3 Wettability of coated filter paper. (a) Photograph of contact angle of water in air (5  $\mu\text{L}$  drop). (b) Photograph of contact angle of oil in air (5  $\mu\text{L}$  drop). In both (a) and (b) no visible drops can be seen – the drops have completed wetted the coated filter paper. (c) Photograph of underwater contact angle of oil (5  $\mu\text{L}$  drop).

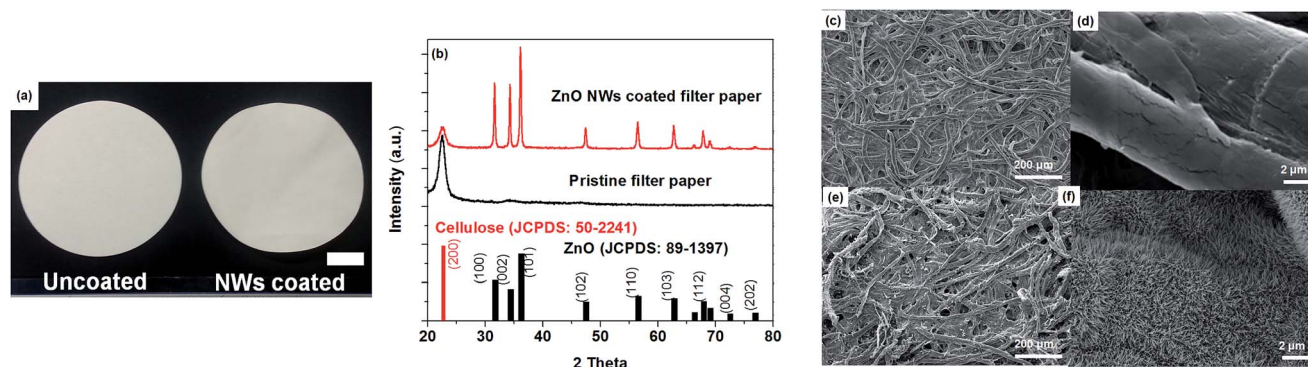


Fig. 2 (a) Optical images of filter paper before (left) and after (right) ZnO NWs coating (scale bar is 2 cm). (b) XRD pattern of uncoated (pristine) and ZnO NWs coated filter paper. (c and d) Secondary electron SEM images of uncoated (pristine) cellulose filter paper with fiber network. (e and f) Secondary electron SEM images of ZnO NWs coated cellulose fibers.



oil to evaluate the underwater oil contact angle due to its higher density than water. The coated filter paper had a large underwater oil contact angle of  $153^\circ$  (Fig. 3c). The underwater superoleophobic property with low oil adhesion is attributed to the rough ZnO NWs and the superhydrophilic ZnO surface,<sup>25,28–30</sup> thus the coating renders an ideal surface condition for gravity driven oil/water separating filter paper.

To further demonstrate the non-fouling characteristics of ZnO NWs coated filter paper, an oil/water selective absorption/desorption processes was demonstrated in Fig. 4. The filter paper was submerged into the oil/water mixture and taken out without any further treatment. After firstly being dipped into the top oil layer, the uncoated filter paper was wetted by oil (kerosene dyed with Oil Red O) due to the large pore size and oleophilic surface. The oil droplets were absorbed (red), which resulted in the formation of an oil fouling layer on the filter surface and blocked the absorption of water due to the difference in surface energy between oil and water (Fig. 4b). However, when the ZnO NWs coated filter paper was submerged into the oil initially, the superoleophobic nature of modified filter paper in water caused a desorption of oil absorption, followed by a full wetting by water, which was dyed with methylene blue, and no visible dyed oil was observed (Fig. 4c).

Fig. 5a and b demonstrate the oil/water separation procedure. The details for experimental setup are described in ESI.† When the surfactant-free oil/water mixture (prepared by mixing water and kerosene at 50 : 50 (v/v)) was poured into the funnel, the superhydrophilic filter paper absorbed water quickly and become saturated, resulting in oil staying at the interface atop the water. Kerosene dyed with Oil Red O was mixed with water and poured into the funnel. Water quickly permeated through

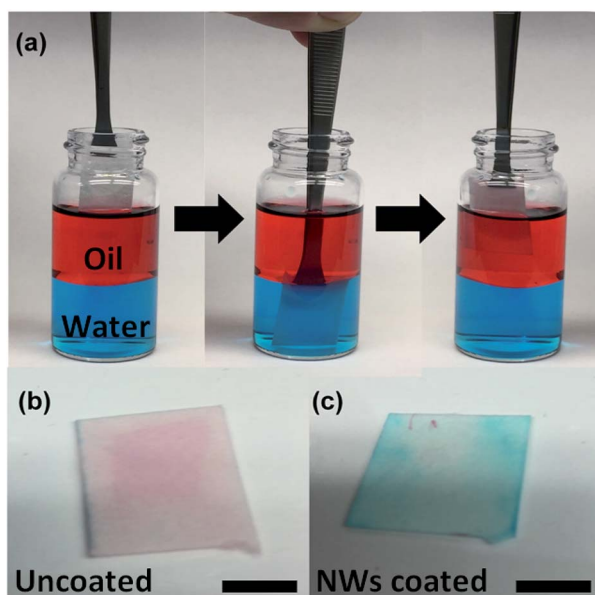


Fig. 4 (a) Demonstration of oil/water selective absorption process. Water was dyed by methylene blue, and oil was dyed by Oil Red O. Optical images of (b) uncoated filter paper after the oil/water absorption – oil was absorbed; (c) ZnO coated filter paper after the oil/water absorption – water was absorbed (scale bar is 1 cm).

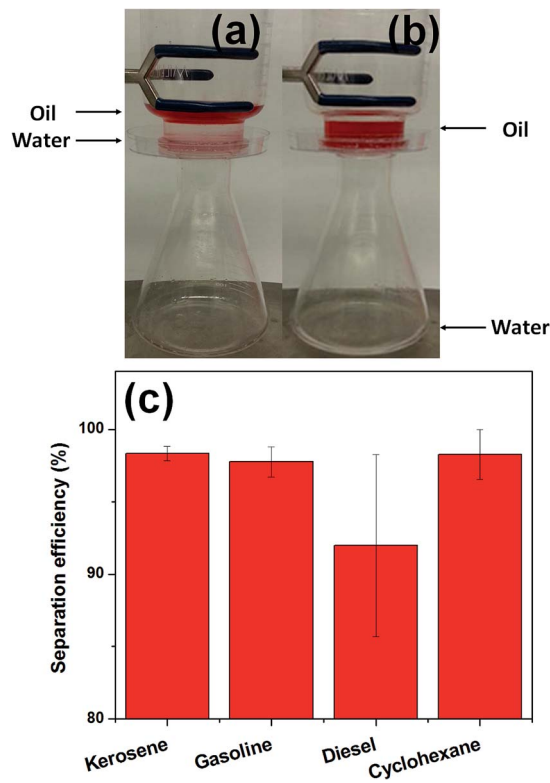


Fig. 5 Photograph of separation test. Digital photo of kerosene (dyed with Oil Red O)/water mixture before (a) and after (b) separation. (c) Separation efficiency of as-prepared filter paper for four different oil/water mixtures.

the filter (in a few minutes) and was collected by the flask below. Meanwhile, oil was retained above the filter paper. No external pressure was applied for the separation and no hints of oil droplets (*i.e.* red dye) were observed within the filtrate. To further determine the oil content in the filtrate after separation, UV-absorption spectra were collected and compared with dyed oil (Fig. S3†).<sup>31,32</sup> There was no discernible dye absorption peak observed from the filtrate, suggesting high purity, selectivity, and effectiveness of the oil/water separation.

To test the oil/water separation of modified filter paper, four types of light oil/water mixtures, including kerosene/water, gasoline/water, diesel/water and cyclohexane/water mixtures were selected. Oil/water separation efficiency was defined as  $m_{\text{separation}}/m_{\text{initial}}$ , where  $m_{\text{separation}}$  is the mass of water after separation, and  $m_{\text{initial}}$  is the mass of water before mixing.<sup>33–36</sup> In all cases, high efficiency values between 91% and 99% were achieved. This result indicates that the modified filter paper was a useful oil/water separator. Moreover, the water flux dependence on different mixtures were also calculated by determining the completely permeated water volume within a certain time period (Fig. S4†). Solely driven by gravity, the filter paper allowed the water flux of 917, 871, 880 and 1060  $\text{L m}^{-2} \text{h}^{-1}$  for kerosene/water, gasoline/water, diesel/water and cyclohexane/water mixtures, respectively. These flux values are comparable to polymeric or ceramic membranes for oil/water mixture separation.<sup>37–40</sup>





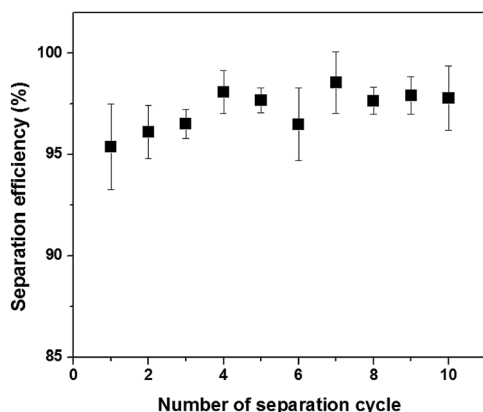


Fig. 6 Cycling performance of the filter paper using kerosene/water mixture.

The recyclability is a key criterion for practical oil/water separation membranes or filters. The separation cycle performance is illustrated in Fig. 6. The filter paper was washed by water after every separation cycle, and dried before the next cycle.<sup>41</sup> For the 10 cycles of sample reutilization, separation efficiency stayed relatively invariant, indicating a prolonged oil anti-fouling property and excellent recyclability.

In summary, superhydrophilic and underwater superoleophobic ZnO NWs coated filter paper was developed by a one pot synthesis method. The hierarchically rough ZnO NWs improved underwater oleophobicity of filter paper, and exhibited anti-fouling oil/water separation properties. The as-prepared filter paper, without further modification, showed high oil/water separation efficiency using gravity and could enable an energy-efficient and environmental-friendly separation process. More importantly, our one pot hydrothermal growth method for ZnO NWs also provides the possibility for scalable fabrication and large scale oil/water separation. Future studies may include the separation of emulsified oil/water mixture. We also note an international standard protocol for reproducible sessile-drop contact angle measurements.<sup>42</sup>

## Acknowledgements

This work is supported by NSERC DG (HJC) & NSERC DG (JAN). Thank you to the NanoFAB at the UofA for imaging and characterization facility usage.

## Notes and references

- 1 J. J. González, L. Viñas, M. A. Franco, J. Fumega, J. A. Soriano, G. Grueiro, S. Muniategui, P. López-Mahía, D. Prada, J. M. Bayona, R. Alzaga and J. Albaigés, *Mar. Pollut. Bull.*, 2006, **53**, 250–259.
- 2 E. Kintisch, *Science*, 2010, **329**, 735–736.
- 3 J. Zhang and S. Seeger, *Adv. Funct. Mater.*, 2011, **21**, 4699–4704.
- 4 A. K. Kota, Y. Li, J. M. Mabry and A. Tuteja, *Adv. Mater.*, 2012, **24**, 5838–5848.

- 5 L. Wen, Y. Tan and L. Jiang, *Angew. Chem., Int. Ed.*, 2015, **54**, 3387–3399.
- 6 B. Wang, W. Liang, Z. Guo and W. Liu, *Chem. Soc. Rev.*, 2015, **44**, 336–361.
- 7 C. Gao, Z. Sun, K. Li, Y. Chen, Y. Cao, S. Zhang and L. Peng, *Energy Environ. Sci.*, 2013, **6**, 1147–1151.
- 8 J. Li, L. Shi, Y. Chen, Y. Zhang, Z. Guo, B. L. Su and W. Liu, *J. Mater. Chem.*, 2012, **22**, 9774–9781.
- 9 L. Feng, Z. Zhang, Z. Mai, Y. Ma, B. Liu, L. Jiang and D. Zhu, *Angew. Chem.*, 2004, **116**, 2046–2048.
- 10 A. K. Kota, J. M. Mabry and A. Tuteja, *Surf. Innovations*, 2013, **1**, 71–83.
- 11 S. J. Gao, Z. Shi, W. B. Zhang, F. Zhang and J. Jin, *ACS Nano*, 2014, **8**, 6344–6352.
- 12 Y. Huang, H. Li, L. Wang, Y. Qiao, C. Tang, C. Jung, Y. Yoon, S. Li and M. Yu, *Adv. Mater. Interfaces*, 2015, **2**, 1400433.
- 13 H. Li, Y. Huang, Y. Miao, W. L. Xu, H. J. Ploehn and M. Yu, *Chem. Commun.*, 2014, **50**, 9849–9851.
- 14 H. Yang, J. Pi, K. Liao, H. Huang, Q. Wu, X. Huang and Z. Xu, *ACS Appl. Mater. Interfaces*, 2014, **6**, 12566–12572.
- 15 F. Zhang, W. B. Zhang, Z. Shi, D. Wang, J. Jin and L. Jiang, *Adv. Mater.*, 2013, **25**, 4192–4198.
- 16 J. J. Wu and S. C. Liu, *Adv. Mater.*, 2002, **14**, 215–218.
- 17 Y. Sun, G. M. Fuge and M. N. R. Ashfold, *Chem. Phys. Lett.*, 2004, **396**, 21–26.
- 18 H. Z. Zhang, X. C. Sun, R. M. Wang and D. P. Yu, *J. Cryst. Growth*, 2004, **269**, 464–471.
- 19 J. Liu, R. Lu, G. Xu, J. Wu, P. Thapa and D. Moore, *Adv. Funct. Mater.*, 2013, **23**, 4941–4948.
- 20 X. Wen, W. Wu, Y. Ding and Z. L. Wang, *J. Mater. Chem.*, 2012, **22**, 9469–9476.
- 21 J. Zhang, L. Sun, J. Yin, H. Su, C. Liao and C. Yan, *Chem. Mater.*, 2002, **14**, 4172–4177.
- 22 K. Liu, W. Wu, B. Chen, X. Chen and N. Zhang, *Nanoscale*, 2013, **5**, 5986–5993.
- 23 M. Law, L. E. Greene, J. C. Johnson, R. Saykally and P. Yang, *Nat. Mater.*, 2005, **4**, 455–459.
- 24 S. H. Ko, D. Lee, H. W. Kang, K. H. Nam, J. Y. Yeo, S. J. Hong, C. P. Grigoropoulos and H. J. Sung, *Nano Lett.*, 2011, **11**, 666–671.
- 25 T. Pauporté, G. Bataille, L. Joulaud and F. J. Vermersch, *J. Phys. Chem. C*, 2010, **114**, 194–202.
- 26 M. Gong, Z. Yang, X. Xu, D. Jasion, S. Mou, H. Zhang, Y. Long and S. Ren, *J. Mater. Chem. A*, 2014, **2**, 6180–6184.
- 27 J. Kim, S. Yun and Z. Ounaies, *Macromolecules*, 2006, **39**, 4202–4206.
- 28 M. Lee, G. Kwak and K. Yong, *ACS Appl. Mater. Interfaces*, 2011, **3**, 3350–3356.
- 29 Z. Cheng, H. Lai, Y. Du, K. Fu, R. Hou, N. Zhang and K. Sun, *ACS Appl. Mater. Interfaces*, 2013, **5**, 11363–11370.
- 30 X. Zheng, Z. Guo, D. Tian, X. Zhang, W. Li and L. Jiang, *ACS Appl. Mater. Interfaces*, 2015, **7**, 4336–4343.
- 31 K. Rohrbach, Y. Li, H. Zhu, Z. Liu, J. Dai, J. Andreasen and L. Hu, *Chem. Commun.*, 2014, **50**, 13296–13299.
- 32 P. Chen and Z. Xu, *Sci. Rep.*, 2013, **3**, 2776.
- 33 J. Li, L. Yan, Y. Zhao, F. Zha, Q. Wang and Z. Lei, *Phys. Chem. Chem. Phys.*, 2015, **17**, 6451–6457.



- 34 Q. Pan, M. Wang and H. Wang, *Appl. Surf. Sci.*, 2008, **254**, 6002–6006.
- 35 X. Jin, B. Shi, L. Zheng, X. Pei, X. Zhang, Z. Sun, Y. Du, J. Kim, X. Wang, S. Dou, K. Liu and L. Jiang, *Adv. Funct. Mater.*, 2014, **24**, 2721–2726.
- 36 Y. Dong, J. Li, L. Shi, X. Wang, Z. Guo and W. Liu, *Chem. Commun.*, 2014, **50**, 5586–5589.
- 37 W. Zhang, Y. Zhu, X. Liu, D. Wang, J. Li, L. Jiang and J. Jin, *Angew. Chem., Int. Ed.*, 2014, **53**, 856–860.
- 38 A. K. Kota, G. Kown, W. Choi, J. M. Mabry and A. Tuteja, *Nat. Commun.*, 2012, **3**, 1025.
- 39 H. Yang, K. Liao, H. Huang, Q. Wu, L. Wan and Z. Xu, *J. Mater. Chem. A*, 2014, **2**, 10225–10230.
- 40 A. Raza, B. Ding, G. Zainab, M. El-Newhy, S. S. Al-Deyab and J. Yu, *J. Mater. Chem. A*, 2014, **2**, 10137–10145.
- 41 M. Tao, L. Xue, F. Kiu and L. Jiang, *Adv. Mater.*, 2014, **26**, 2943–2948.
- 42 J. Drelich, *Surf. Innovations*, 2013, **1**, 248–254.

